JOURNAL OF SOLID STATE CHEMISTRY 113, 272–280 (1994)

A TEM and Group Theoretical Study of α-PbO and Its Low-Temperature Improper Ferroelastic Phase Transition

Ray L. Withers[1] and Siegbert Schmid

Research School of Chemistry, Australian National University, Canberra, Australian Capital Territory 0200, Australia

Received October 19, 1993; accepted February 18, 1994

The results of a detailed TEM and group theoretical study of α-PbO and its low-temperature, improper ferroelastic phase transition are reported. Ferroelastic twinning of the low-temperature, incommensurately modulated phase is observed and typically found to be on a scale rather less than 1 μm. Some unusual features of the reciprocal space of this low temperature phase are reported including the coexistence of sharp incommensurate satellite reflections and a closely related diffuse intensity distribution as well as the presence of "bands" of diffuse intensity absence along $\{hkh\}^*$ directions of reciprocal space. Single domain electron diffraction patterns of the low-temperature incommensurately modulated phase are found to be incompatible with a previously reported structure refinement and to require a 4-dimensional superspace group symmetry of $P : Cmma : s, -1, 1$. The most general possible atomic displacement pattern compatible with this symmetry is derived from group theoretical considerations.

1. INTRODUCTION

The discovery of a low-temperature, incommensurate, improper ferroelastic phase transition in the vicinity of 220 K (1–6) has prompted much recent study of the tetragonal, or α, form of PbO (see Fig. 1). The improper ferroelastic nature of this transition, rather than its incommensurate character, provided the initial reason for its discovery (5). It was not long, however, before the appearance of additional incommensurate satellite reflections below the second order phase transition was noted (1). The condensation of a small amplitude, incommensurate $\mathbf{q} = \alpha(-\mathbf{a}_t^* + \mathbf{b}_t^*) \sim 0.185(-\mathbf{a}_t^* + \mathbf{b}_t^*)$ displacive modulation of the $P4/nmm$ ($\mathbf{a}_t$, $\mathbf{b}_t$, $\mathbf{c}_t$) parent structure at the phase transition means that the tetragonal $(110)_t^*$ and $(1, -1, 0)_t^*$ directions of reciprocal space are no longer equivalent. Hence the transition is also accompanied by an infinite wavelength strain wave which very weakly breaks the parent tetragonal symmetry (5) and lowers the average structure space group symmetry from $P4/nmm$ ($\mathbf{a}_t$, $\mathbf{b}_t$, $\mathbf{c}_t$) to $Cmma$ ($\mathbf{a} = (\mathbf{a}_t + \mathbf{b}_t)$, $\mathbf{b} = (-\mathbf{a}_t + \mathbf{b}_t)$, $\mathbf{c} = \mathbf{c}_t$).

[1] To whom correspondence should be addressed.

The magnitude of this ferroelastic distortion is very small (<0.1%; Ref. (1)) and is not detectable in conventional selected area electron diffraction patterns (SADPs).

Moreau *et al.* (1) also observed a significant diffuse background in neutron powder diffraction profiles at room temperature and suggested that the appearance of the low-temperature ferroelastic phase was strongly correlated with the disappearance of the diffuse intensity as temperature was lowered. In a preliminary TEM study (6), it was shown that this room temperature diffuse intensity distribution took the form of discs perpendicular to the $\{110\}_t^*$ directions of reciprocal space and corresponded to a characteristic "tweed" microstructure (minimum dimension ~15 Å) in real space. On the basis of $\{110\}_t^*$ systematic row electron diffraction patterns, it was suggested that "tweed" in α-PbO could be satisfactorily described in terms of pure "transverse distortion waves" and that the atomic displacements responsible for the diffuse streaking were very closely related to those associated with the long-range-ordered incommensurate modulation which freezes in at lower temperatures.

The only reported structure refinement (2) of this low-temperature incommensurately modulated phase (from X-ray and neutron powder diffraction data), however, reported a 4-dimensional superspace group symmetry of $P:C2mb:-1,-1,1$. The atomic displacement pattern associated with the incommensurate primary modulation wave-vector $\mathbf{q} \sim 0.37\mathbf{b}^*$ was reported to require significant Pb and O motion along all three orthorhombic directions including $\mathbf{b}$ in apparent conflict with the previously reported $\{110\}_t^*$ and $(020)^*$ systematic row electron diffraction patterns (6), i.e., clearly not a condensed transverse distortion wave! The prime motivations for the present work were, first to determine via TEM the appropriate superspace group symmetry and corresponding symmetry-allowed atomic displacement pattern of the low-temperature incommensurately modulated phase and, second to present the results of a detailed TEM study of α-PbO.

0022-4596/94 $6.00

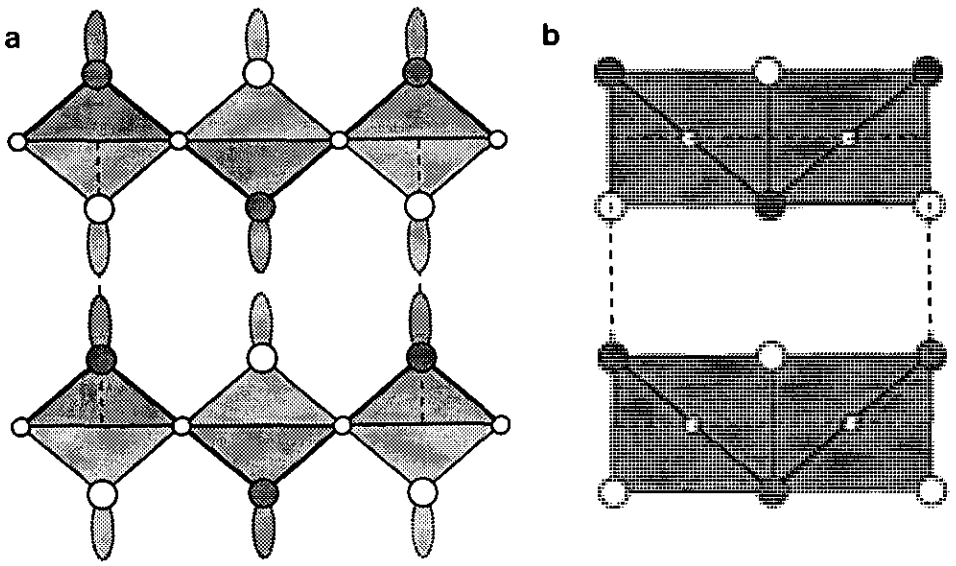

FIG. 1. Alternative polyhedral representations of the room temperature $P4/nmm$ tetragonal α-PbO structure projected along a $\langle 110\rangle_t$ direction: the orthogonal $\langle 110\rangle_t$ direction is horizontal and the $[001]_t$ direction vertical. Large circles represent Pb atoms (open and hatched at projected heights of 0 and $\frac{1}{2}$, respectively), while the smaller open circles represent oxygen atoms (at projected heights of $\frac{1}{4}$ and $\frac{3}{4}$). In (a) the coordination of the Pb atoms is emphasized (the lone pairs on the Pb atoms are represented by lobes), while in (b) the edge-connected $\{OPb_4\}$ tetrahedral coordination of the oxygens is emphasized. The projected unit cell is outlined.

2. EXPERIMENTAL

Thermal decomposition of β-PbO_2 (BDH Chemicals, >95%) under a nitrogen atmosphere for 2 hr at 600°C was used to prepare a well-crystallized sample of α-PbO. The course of the decomposition was monitored by X-ray powder diffraction (XRD) using a Guinier–Hägg camera with monochromated Cu$K\alpha_1$ radiation. Unit cell dimensions were determined using Si (NBS No. 640) as an internal standard.

TEM specimens were initially prepared simply by grinding and dispersing on to a holey carbon film. Because of the layered nature of α-PbO, however, this invariably produced grains with the **c**-axis oriented along the beam direction. In order to obtain diffraction patterns with the **c***-axis excited, it was necessary to embed the powdered specimen in epoxy, cut and polish an appropriate thin section, and then finally thin the section further with an ion beam. The resultant specimens were examined in JEOL 100CX and Philips EM430 electron microscopes. The low-temperature work utilized a Gatan 636N liquid-nitrogen cold stage.

3. RESULTS

3.1. Powder XRD

The refined unit cell parameters for the room temperature α-PbO specimen were $a_t = b_t = 3.9719(3)$ Å, $c = 5.023(1)$ Å, space group $P4/nmm$; $V = 79.25$ Å^3. These values are in good accord with those reported by Moreau *et al.* (1).

3.2. Electron Diffraction

Figure 2 shows typical (a) [100], (b) [010], and (d) ~[001] zone axis microdiffraction patterns taken below the incommensurate phase transition, while (c) is a typical [001] zone axis SADP. Note that the microdiffraction patterns are taken from much smaller areas (~a few hundred Å in diameter) than the typical area illuminated in order to obtain the SADPs (i.e., ~1 μm in diameter). Such spatial resolution is necessary if diffraction patterns from nontwinned regions, i.e., from a single ferroelastic domain, are to be obtained.

SADPs (see Figs. 2c and 4a) often include both ferroelastic domains and hence appear to show incommensurate satellite reflections along both of the parent $\{110\}_t^*$ directions. With the aid of microdiffraction patterns and careful probe positioning (see Fig. 2d, for example), however, it can be shown that the incommensurate satellite reflections occur along only one of the two local $\{110\}_t^*$ directions (i.e., along the **b*** direction of the strain-distorted *Cmma* average structure reciprocal lattice), confirming the single-**q** nature of the phase transition (1) and providing a structural mechanism for the improper ferroelastic behavior at the phase transition. That SADPs almost invariably show satellite reflections along both parent $\{110\}_t^*$ directions indicates that the typical size of the ferroelastic domains must be rather less than 1 μm.

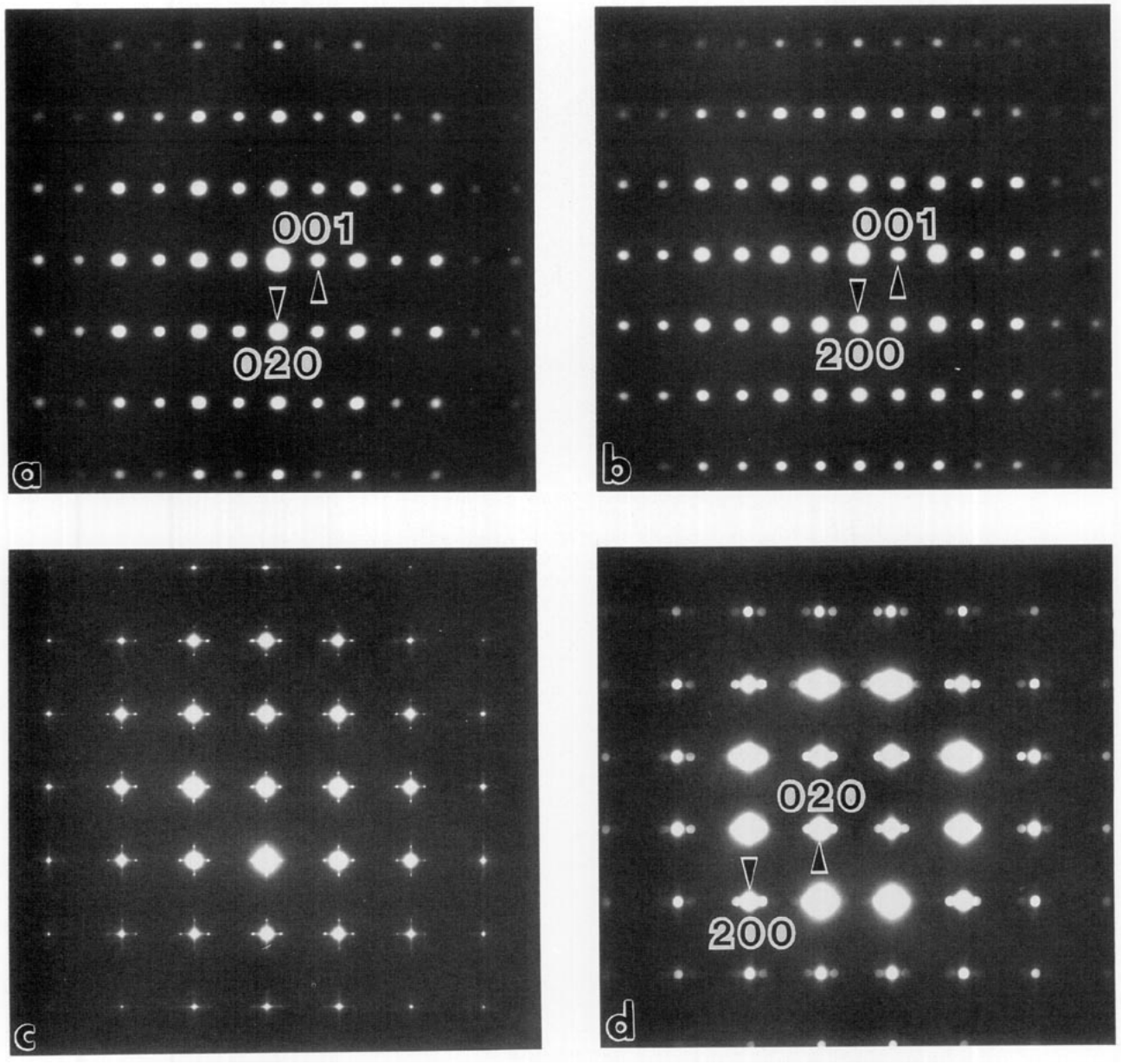

FIG. 2. Shows typical (a) [100], (b) [010], and (d) ~ [001] zone axis microdiffraction patterns taken below the incommensurate phase transition. (c) is a typical [001] zone axis selected area electron diffraction pattern (SADP).

Given this problem with twinning, one might think that it would be extremely difficult to distinguish [100] from [010] diffraction patterns. While this is true if only zero order Laue zone (ZOLZ) reflections are taken into account, it is no longer true if the higher OLZ (HOLZ) reflections are taken into account. Thus, in the case of the [010] zone axis, a weak superlattice HOLZ ring (see Fig. 3) is always present. This superlattice HOLZ ring, however, disappears at a [100] zone axis and hence provides a characteristic signature, enabling [010] and [100] zone axis orientations to be readily distinguished. The absence of satellite reflections in the ZOLZ of [100] diffraction patterns is consistent with the absence of satellite reflections along the **b*** direction in (020)* systematic row SADPs as previously reported (6) and confirms the pure transverse distortion wave model (see Section 4 below). Such an extinction condition is very significant and clearly demonstrates that the previously reported superspace group symmetry ($P{:}C2mb{:}-1,-1,1$) and structure of low-temperature α-PbO (2) cannot be correct.

The very characteristic diffuse streaking of the room temperature structure, while much diminished in inten-

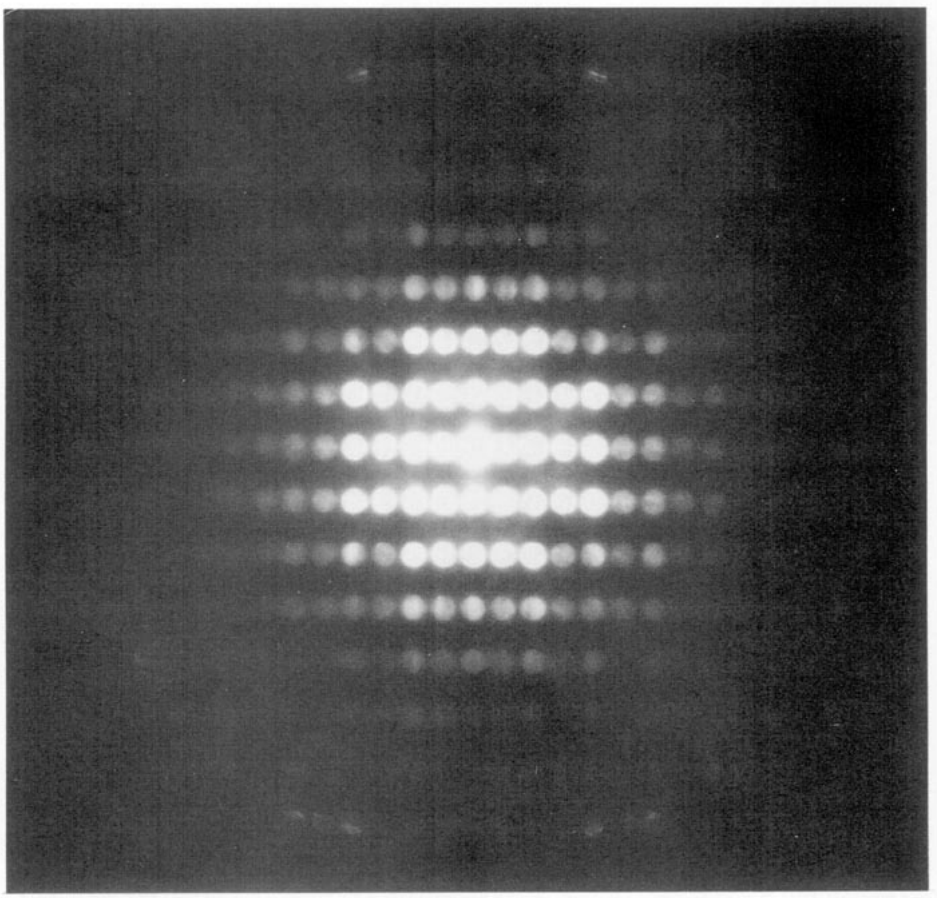

FIG. 3. Shows a typical [010] zone axis convergent beam electron diffraction pattern (CBP). Indexing is as in Fig. 2b. The weak superlattice HOLZ ring provides a characteristic signature enabling [100] and [010] zone axis orientations to be distinguished.

sity, does not disappear altogether at the incommensurate phase transition as is most clear from zone axis SADPs such as the ⟨1, −1, 2⟩ zone axis SADP shown in Fig. 4a and the corresponding zone axis SADP from the room-temperature phase shown in Fig. 4b. Note that the incommensurate satellite reflections do not occur in the ZOLZ at this ⟨1, −1, 2⟩ zone axes, but rather are slightly out of the plane and hence show up in the form of a satellite HOLZ ring on the edge of the pattern shown in Fig. 4a. That the higher temperature diffuse intensity distribution, while reduced in intensity, nonetheless continues to coexist with the long-range-ordered incommensurate modulation below the completely reversible phase transition at ~220 K is also characteristic of, for example, the $1T$ to $1T_1$ phase transitions of TaS_2 and $TaSe_2$ (7) and raises interesting questions as to how "phason disorder" in such incommensurately modulated structures should be taken into account.

A similarly intriguing feature of the reciprocal lattice of the low-temperature incommensurately modulated phase is the presence of polarized "bands" of diffuse intensity absence running along the $(h, k, -h)^*$ and $(hkh)^*$ directions of reciprocal space—see, for example, those arrowed in Fig. 5 and running along the $(2, 0, -2)^*$ and $(202)^*$ directions of reciprocal space. Tilting experiments show that such "bands" of diffuse intensity absence form part of a planar slab of diffuse absence characterized by vector normals of [101] and [1, 0, −1], respectively. The presence of such polarized "bands" of diffuse intensity absence and the asymmetry of the corresponding diffraction effect, i.e., the transfer of diffuse intensity from the low to the high angle side of the neighboring rows of strong Bragg reflections (see Fig. 5), is strongly reminiscent of the diffraction effects characteristic of the so-called "atomic size effect" (8–10).

The atomic size effect first arose in the context of binary, substitutionally disordered alloys in which two atoms of different size occupy a single sublattice. The interaction between short-range compositional ordering on this sublattice and the associated displacive relaxation gives rise to characteristic diffraction effects such as the existence of planes of diffuse intensity absence perpen-

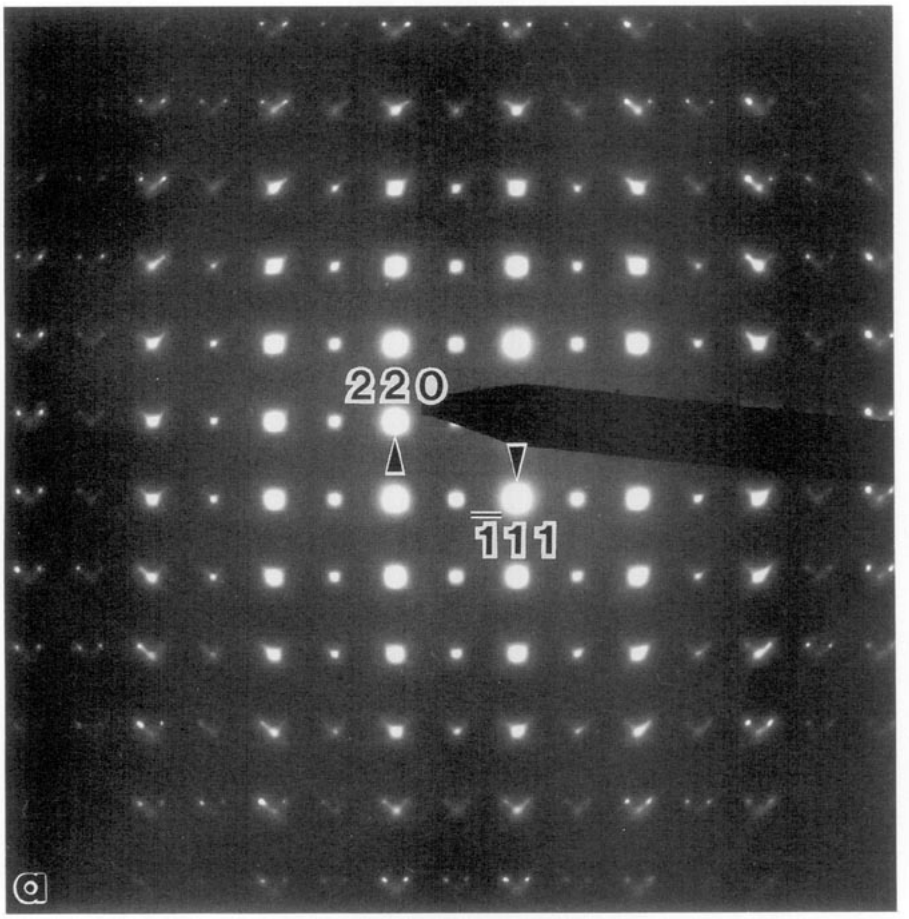

FIG. 4. Shows (a) a typical $\langle 1, -1, 2\rangle$ zone axis SADP of the low-temperature incommensurate phase along with (b) the corresponding SADP from the room-temperature phase.

dicular to directions connecting nearest neighbor atoms and the asymmetric transfer of diffuse intensity from regions on one side of Bragg reflections to regions on the other (9–10). In our case, however, it would appear that no such compositional disorder on a particular sublattice exists although the normals to the observed planes of diffuse absence do correspond to directions connecting nearest neighbor Pb atoms (see Fig. 1b). Presumably the short-range displacive disorder associated with the diffuse streaking (see Fig. 4a) plays some role analogous to the compositional disorder in the classical size effect. Further consideration, however, is beyond the scope of the current paper. Clearly, more theoretical and experimental work will need to be carried out in order to understand the origin of this intriguing diffraction feature of low-temperature α-PbO.

3.3. Electron Microscopy

Figure 6 shows a typical medium-resolution lattice image of the low-temperature incommensurately modulated phase taken tilted a few degrees away from the [001] zone axis in such a way that a $\{110\}^*$ reflection is strongly excited. The objective aperture allowed only the straight-through beam plus the surrounding incommensurate satellite reflections to contribute to the corresponding image. Fringes separated by ~15 Å and corresponding to the inverse of the incommensurate modulation wave-vector are clearly visible over the whole of the field of view (~0.2 × 0.17 μm in area).

In some areas (e.g., in the vicinity of that labeled A in Fig. 6) only fringes running vertically (i.e., single-**q** regions) are observed, while in other areas (e.g., that labeled C) both horizontal and vertical fringes coexist. There are two possible interpretations of such contrast. The first is that this region corresponds to a double-**q** state of different structure to the clearly single-**q** regions. This however seems very unlikely. Rather than attribute this contrast to a double-**q** state, we interpret the apparent coexistence of horizontal and vertical fringes in regions such as this as being due to the presence of an

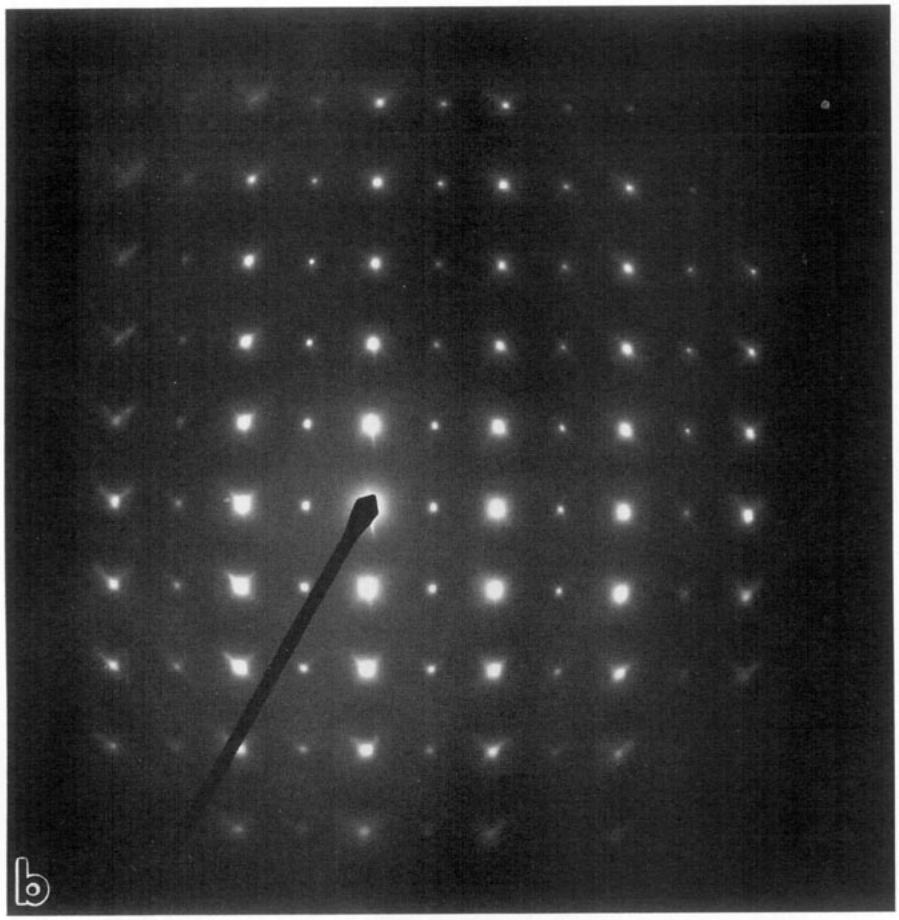

FIG. 4—*Continued*

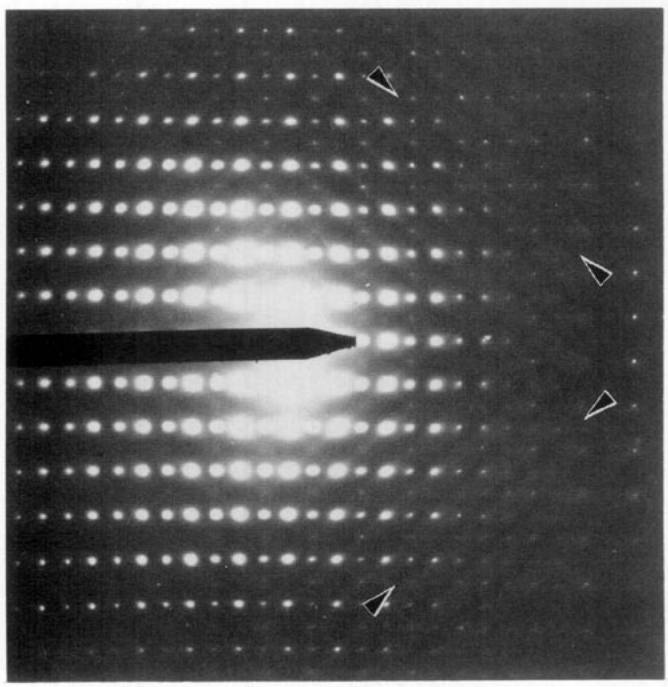

undetected twin boundary perpendicular to the **c**-direction somewhere through the foil thickness.

The larger scale heterogeneous defect structures also visible in Fig. 6 sometimes (as at B) clearly perturb the superlattice fringes and sometimes (as at A) do not. The presence of both horizontal and vertical fringes within the $\sim 0.2 \times 0.17$ μm area shown in Fig. 6 is typical and is consistent with the difficulty previously mentioned in obtaining SADPs from a single ferroelastic domain. Occasionally, however, rather larger single-**q** domain regions (as shown by the existence of only a single set of ~15 Å fringes and the presence of only a single set of satellite reflections in the corresponding SADP (inset)) can be found as shown in Fig. 7.

FIG. 5. An SADP of the low-temperature incommensurate phase taken tilted slightly away from exact [010] zone axis orientation. Indexing of the ZOLZ is again as in Fig. 2b. Note the polarized bands of diffuse intensity absence (arrowed) running along the (2, 0, −2)* and (202)* directions of reciprocal space.

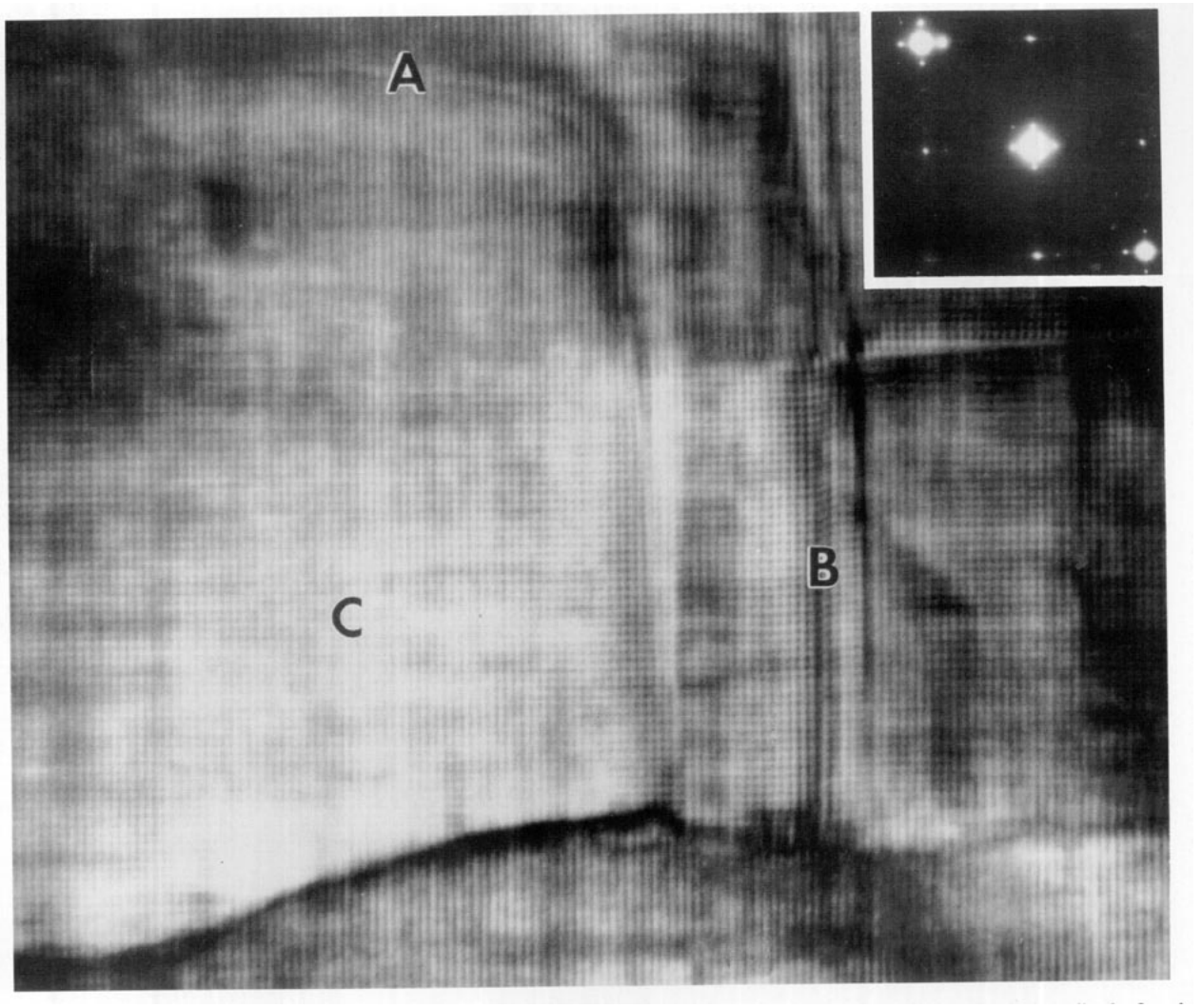

FIG. 6. A typical ~130K medium-resolution lattice image of the low temperature incommensurately modulated phase taken tilted a few degrees away from the [001] zone axis in such a way that a {110}* reflection is strongly excited. The corresponding SADP is inset. Fringes separated by ~15 Å and corresponding to the inverse of the incommensurate modulation wave-vector are clearly visible. In some areas (e.g., in the vicinity of that labeled A in Fig. 6) only fringes running vertically are observed, while in other areas (e.g., that labeled C) both horizontal and vertical fringes coexist.

4. GROUP THEORETICAL CONSIDERATIONS

The observed characteristic extinction conditions (see Fig. 2) of the low-temperature incommensurately modulated phase

$$F(hklm)^* = 0 \text{ unless } h + k = 2n$$
$$F(hk0m)^* = 0 \text{ unless } h, k = 2n$$
$$\text{and } F(0klm)^* = 0 \text{ unless } m = 2n$$

require a 4-dimensional superspace group symmetry of at least $P : Cm2a : ss1$ but most probably $P : Cmma : s, -1, 1$ following the general notation of de Wolff *et al.* (11). (Note that these superspace groups will not be found in the tables of (11), as the authors there followed a convention that the primary modulation wave-vector should be along a **c***-direction). The absence of satellite reflections in the ZOLZ of [100] zone axis SADPs (see Fig. 2a) is clearly incompatible with the previously reported superspace group symmetry of $P : C2mb : -1, -1, 1$ (2). Note, however, that $P : C2mb : -1, -1, 1$ is a subgroup of $P : Cmma : s, -1, 1$.

4.1. The Average or Reference Structure

The symmetry-allowed atomic displacement pattern associated with the primary modulation wave-vector (in this case $\mathbf{q} = 2\alpha\mathbf{b}^* \sim 0.37\mathbf{b}^*$) can now be described in

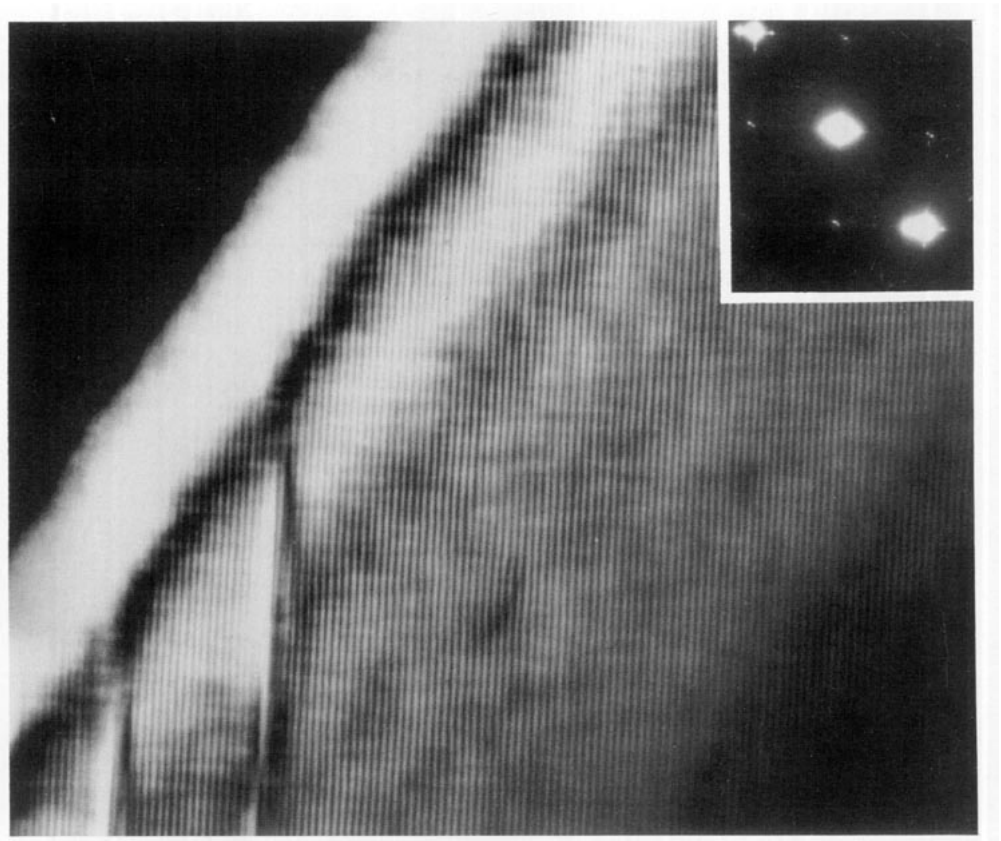

FIG. 7. An ~130K medium-resolution image of a large single-**q** region again taken tilted a few degrees away from the [001] zone axis in such a way that a {110}* reflection is strongly excited. (The corresponding *SADP* is inset).

terms of displacive modulation of a reference structure which can be taken to be the strain-deformed *Cmma* ($\mathbf{a} = \mathbf{a}_t + \mathbf{b}_t$, $\mathbf{b} = -\mathbf{a}_t + \mathbf{b}_t$, $\mathbf{c} = \mathbf{c}_t$) average structure (see Fig. 8 and Ref. (5)). There are two Pb atoms (labeled Pb1 and Pb2, respectively) and two O atoms (labeled O1 and O2, respectively) per primitive unit cell of this reference structure with fractional coordinates given by 0, 0, z; 1/2, 0, $-z$ and $-1/4$, 1/4, 0; 1/4, 1/4, 0, respectively.

4.2. Irreducible Representations and Atomic Displacement Pattern Associated with the Primary Modulation Wave-Vector $\mathbf{q} = 0.37\mathbf{b}^*$

The little co-group (see Chap. 3 of (12)) of the primary modulation wave-vector $\mathbf{q} = 0.37\mathbf{b}^*$ is that subgroup of *mmm* which leaves **q** invariant modulo an allowed matrix reflection, namely $\{E, \sigma_x, C_{2y}, \sigma_z\}$. The multiplication table corresponding to this little cogroup is given below:

	E	σ_x	C_{2y}	σ_z
R_1	1	1	1	1
R_2	1	−1	1	−1
R_3	1	1	−1	−1
R_4	1	−1	−1	1

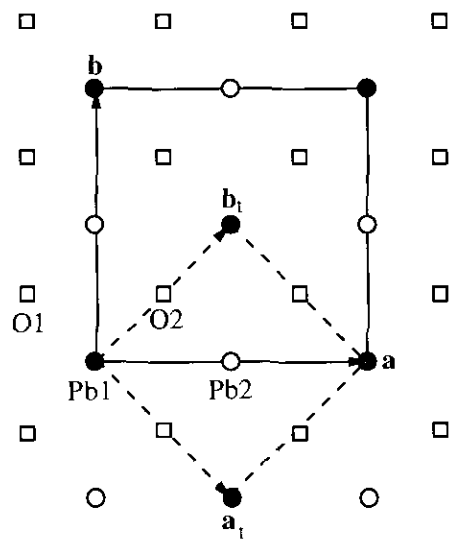

FIG. 8. The *P4/nmm* tetragonal α-PbO structure projected along the $[001]_t$ direction: the $\mathbf{a}_t$ and $\mathbf{b}_t$ basal plane axes appropriate to the room-temperature structure are shown along with the enlarged average structure basal plane axes ($\mathbf{a} = \mathbf{a}_t + \mathbf{b}_t$, $\mathbf{b} = -\mathbf{a}_t + \mathbf{b}_t$) appropriate for the average structure of the low-temperature phase. Pb atoms are represented by circles (open at $+z$, filled at $-z$), while the oxygen atoms (at height $z = 0$) are represented by the open squares. The four Bravais lattice independent sites are labeled Pb1, Pb2, O1, and O2, respectively.

A superspace group symmetry of $P : Cmma : s, -1, 1$ requires odd-order harmonics to transform with R_4 symmetry and even-order harmonics to transform with R_1 symmetry. As only the first harmonic is ever observed in practice, however, it is not necessary to consider any harmonic order other than the first. The previously reported superspace group symmetry of $P:C2mb : -1, -1, 1$ (2), a subgroup of $P : Cmma : s, -1, 1$, allows harmonics to transform with more than one symmetry simultaneously; e.g., odd-order harmonics can transform with both R_4 and R_1 symmetry. Such a phase transition would be extremely unusual and, as shown by the observed extinction conditions (see Fig. 2), does not occur.

Application of standard group theoretical techniques (see, for example, (13)) gives the most general possible atomic displacement pattern associated with this modulation wave-vector $\mathbf{q} = 2\alpha\mathbf{b}^* \sim 0.37\mathbf{b}^*$ as

$$\mathbf{u}_{\mathrm{Pb}1}(\mathbf{T}) = \mathbf{u}_{\mathrm{Pb}2}(\mathbf{T}) = \varepsilon_{\mathrm{Pb}}(x)\,\mathbf{a}\cos(2\pi\mathbf{q}\cdot\mathbf{T} + 90^\circ + \theta)$$

$$\mathbf{u}_{\mathrm{O}1,2}(\mathbf{T}) = \varepsilon_0(x)\,\mathbf{a}\cos(2\pi\mathbf{q}\cdot\mathbf{T} + 90^\circ + \pi\alpha + \theta) \pm \varepsilon_0(z)\,\mathbf{c}\cos(2\pi\mathbf{q}\cdot\mathbf{T} + \pi\alpha + \theta).$$

Note that the symmetry-allowed atomic displacement pattern is purely transverse; i.e., there are no atomic shifts allowed along the direction of the modulation wave-vector, contrary to the results of (2). Thus there are only three independent displacive degrees of freedom to be determined, namely $\varepsilon_{\mathrm{Pb}}(x)$, $\varepsilon_0(x)$, and $\varepsilon_0(z)$. The anisotropic thermal parameters for Pb and O obtained from the 2K average structure refinement of Boher *et al.* (5) are consistent with the above proposed atomic displacement pattern and would suggest magnitudes for the above parameters ~0.02 corresponding to ~0.1 Å magnitude shifts.

5. CONCLUSIONS

In conclusion, the observed SADPs of low-temperature α-PbO are not compatible with the previously reported superspace group symmetry and structure (2) and suggest the need for re-refinement. The reason for this discrepancy is not at all obvious to us, although it would seem that the continued existence of the characteristic room-temperature diffuse intensity distribution in the low-temperature, incommensurately modulated phase (see Fig. 4) (i.e., the coexistence of both sharp incommensurate satellite reflections and the closely related characteristic diffuse streaking) may well play an important role.

ACKNOWLEDGMENT

The authors acknowledge fruitful discussions with Dr. John Fitz Gerald.

REFERENCES

1. J. Moreau, J. M. Kiat, P. Garnier, and G. Calvarin, *Phys. Rev. B* **39,** 10296 (1989).
2. A. Hedoux, D. Grebille, and P. Garnier, *Phys. Rev. B* **40,** 10653 (1989).
3. K. Chhor, C. Pommier, P. Garnier, and L. Abello, *J. Phys. Chem. Solids* **52,** 895 (1991).
4. D. Le Bellac, J. M. Kiat, A. Hedoux, P. Garnier, D. Grebille, Y. Guinet, and I. Noiret *Ferroelectrics* **125,** 215 (1992).
5. P. Boher, P. Garnier, J. R. Gavarri, and A. W. Hewat, *J. Solid State Chem.* **57,** 343 (1985).
6. R. L. Withers, S. Schmid, and J. D. Fitz Gerald, *in* "Defects and Processes in the Solid State: Geoscience Applications: The McLaren Volume" (J. N. Boland and J. D. Fitz Gerald, Eds.), pp. 305–316. Elsevier, Amsterdam, 1993.
7. R. L. Withers and T. R. Welberry, *J. Phys. C* **20,** 5975 (1987).
8. B. E. Warren, B. L. Averbach, and B. W. Roberts, *J. Appl. Phys.* **22,** 1493 (1951).
9. B. D. Butler, R. L. Withers, and T. R. Welberry, *Acta Crystallogr. Sect. A* **48,** 737 (1992).
10. T. R. Welberry, *J. Appl. Crystallogr.* **19,** 382–389 (1986).
11. P. M. de Wolff, T. Janssen, and A. Janner, *Acta Crystallogr. Sect. A* **37,** 625 (1981).
12. C. J. Bradley and A. P. Cracknell, "The Mathematical Theory of Symmetry in Solids." Clarendon Press, Oxford, 1972.
13. R. L. Withers, R. Wallenberg, D. J. M. Bevan, J. G. Thompson, and B. G. Hyde, *J. Less-Common Met.* **156,** 17 (1989).